Sediment source apportionment using geochemical composite signatures in a large and polluted river system with a semiarid-coastal interface, Brazil

Rennan Cabral Nascimento, Angelo Jamil Maia, Ygor Jacques Agra Bezerra da Silva, Fábio Farias Amorim, Clístenes Williams Araújo Do Nascimento, Tales Tiecher, O. Evrard, Adrian Collins, Caroline Miranda Biondi, Yuri Jacques Agra Bezerra da Silva

Sediment source apportionment using geochemical composite signatures in a large and polluted river system with a semiarid-coastal interface, Brazil

Rennan Cabral Nascimento[a], Angelo Jamil Maia[a], Ygor Jacques Agra Bezerra da Silva[a], Fábio Farias Amorim[a], Clístenes Williams Araújo do Nascimento[a], Tales Tiecher[b], Olivier Evrard[c], Adrian L. Collins[d], Caroline Miranda Biondi[a], Yuri Jacques Agra Bezerra da Silva[e]

[a]Agronomy Department, Federal Rural University of Pernambuco (UFRPE), Dom Manuel de Medeiros Street, s/n - Dois Irmãos, 52171-900 Recife, PE, Brazil
[b]Department of Soil Science, Federal University of Rio Grande do Sul (UFRGS), Interdisciplinary Research Group on Environmental Biogeochemistry (IRGEB), Bento Gonçalves Ave. 7712, 91540-000 Porto Alegre, RS, Brazil
[c]Laboratoire des Sciences du Climat et de l'Environnement (LSCE/IPSL), Unité Mixte de Recherche 8212 (CEA-CNRS-UVSQ), Université Paris-Saclay, Gif-sur-Yvette, France
[d]Net Zero and Resilient Farming, Rothamsted Research, North Wyke, Okehampton EX20 2SB, UK
[e]Agronomy Department, Federal University of Piauí (UFPI), Planalto Horizonte, 64900-000 Bom Jesus, PI, Brazil

Abstract

The Ipojuca River is the third most polluted fluvial system in Brazil. Sediment-associated metal fluxes threaten the environmental health in the estuary of this system. However, the sources supplying these particle-bound contaminants have not been determined yet. Sediment source fingerprinting provides a powerful technique to obtain such information. Accordingly, the aim of this study was to quantify the source contributions to suspended and bed sediments in this polluted river system with a semiarid-coastal interface using geochemical tracers. A total of 20 geochemical tracers measured on 207 source samples were used as potential fingerprint properties to discriminate and quantify the contributions of potential sources classified according to three distinct typologies (distribution of land uses, soil classes, and the environmental contrasts between the upper and lower catchment). All analyzed elements passed the range test for conservative behaviour. Using the MixSIAR model, the lower catchment, Oxisols, and sugarcane croplands were identified as the dominant sediment sources. These new data provide a basis to target the management of excessive sediment loads and sediment-associated contaminants moving towards estuarine and coastal environments. The multiple sources framework discussed herein can also help to improve the appeal of sediment source fingerprinting among environmental policymakers given the capacity for informing targeted management.

Keywords: soil erosion; sediment source fingerprinting; multiple sources framework; Bayesian un-mixing model

1. Introduction

In Brazil, high erosion rates have often been associated with changes in land cover, due to the expansion of agriculture, and with the implementation of inappropriate practices of soil management, such as up and down slope farming without terraces and use of heavy agricultural machinery (Didoné et al., 2015). Events with high rainfall intensities occur frequently in this part of the world (Anache et al., 2017). Combined, these conditions can generate elevated volumes of surface runoff and high sediment loads in river systems across the country (Molisani et al., 2006; Strauch et al., 2013). In this context, it is fundamental to obtain reliable information on the origin of sediment in order to improve our understanding of key controlling processes and to support targeted mitigation plans.

The sediment fingerprinting approach is increasingly used worldwide (Haddadchi et al., 2013; Collins et al., 2020). In brief, this approach involves the comparison of conservative bio-physico-chemical properties of sediment source and target sediment samples to determine the relative contributions of individual sources through the application of statistical tests and numerical mass balance modelling (Walling et al., 1999; Collins et al., 2010). The critical requirements for robust applications of the fingerprinting approach have been discussed in Collins et al. (2017).

In large river catchments, the heterogeneous environmental features (i.e., geology, pedology, geomorphology and climate) can challenge the robust geochemical characterization of potential individual sediment sources. This, in turn, can undermine robust land use-based source discrimination and consequently generate more substantive errors for sediment source apportionment (Pulley et al., 2017). To avoid these difficulties, sediment source apportionment based on soil type may provide a pragmatic alternative, since soils express geochemical signatures inherited from the parent material and pedogenetic processes. For instance, soils with elevated weathering rates tend to exhibit higher contents of low mobility chemical elements, such as Al, Ti, Si, Th, Zr, and Fe, and lower contents of high mobility chemical elements, such as K, Na, Cl, Mg, and Ca, compared to less weathered soils (Silva et al., 2020). Nevertheless, the geochemical potential for source classification according to soil type has received little attention in the literature so far in comparison with land use (Evrard et al., 2013; Lepage et al., 2016; Le Gall et al., 2016; Silva et al., 2018a). Another alternative is the recent work of Batista et al. (2019), who developed a regional source classification based on the interpretation of lithological and soil maps, and the *a priori* knowledge of erosion processes in a large river

basin of Minas Gerais, Southeastern Brazil. They divided the catchment into different parts (upper, middle and lower), revealing more robust discriminations (90% of source samples classified correctly) using the geochemical composition of particles <63 μm. Most importantly, few studies have assessed different strategies to classify and quantify different sediment sources in the same river catchment - a relevant step to providing well-designed policies and control strategies for protecting soil and water resources, especially in large complex catchments (Pulley et al., 2017).

The Ipojuca River catchment is considered to be one of the most polluted river systems and the third worst for water quality indices in Brazil (IBGE, 2015). Surveys have linked high loads of metals and natural radionuclides transported in suspended sediment to natural hotspots and to battery factories, textile industries and some municipalities that directly discharge non-treated wastewater into the upstream river (Lima Barros et al., 2013; Silva et al., 2015; Silva et al., 2018b; Nascimento et al., 2019). The construction of a Harbour Complex and dams near the estuary in the 1980s have decreased the hydrological connectivity at the estuary-sea interface. Accordingly, the control of erosion and sediment delivery in these fragile ecosystems requires a better understanding of sediment transfer processes in these areas. To this end, the current research provides one of the first sediment fingerprinting studies conducted in the Northeastern region of Brazil. In this work, we assessed the apportionment patterns of different sediment source typologies (soil type, land use, and catchment zone) in the Ipojuca River catchment using a suite of geochemical tracers. The implications of these novel results for supporting the environmental recovery of this polluted river basin and its coastal environments are then discussed.

2. Materials and methods

2.1 Study area

The Ipojuca River catchment (08 ° 09 ′ 50 ″ - 08 ° 40 ′ 20 ″ S and 34 ° 57 ′ 52 ″ S and 34 ° 57 ′ 52 ″ - 37 ° 02 ′ 48 ″ W; Fig. 1) extends from the western semiarid zone to the humid coast of Pernambuco State, Northeastern Brazil. The total area of the catchment is ~3435 km² and the main watercourse is 324 km long (CONDEPE / FIDEM, 2005). The depth and width of downstream cross-sections of the main watercourse vary from 0.8 to 2.4 m and 21.8 to 30.3 m, respectively. Flow rates and suspended sediment discharge for the same section vary from 1.2 to 25 $m^3 s^{-1}$ and 7.6 to 669 Mg day^{-1} in periods of low and high flow rate, respectively (Silva et al., 2015).

The mean annual rainfall ranges from 600 to 800 mm in the semiarid upstream part with high spatial and temporal variability, and from 1800 to 2400 mm in the downstream coastal zone where the rain is distributed more evenly throughout the autumn-winter months. These different patterns of rain distribution promote an intermittent fluvial regime in the upstream reaches, and a perennial regime in the middle to downstream reaches. The local average air temperature varies from 25 to 28 °C; typical of Brazilian tropical conditions (CONDEPE / FIDEM 2005). Undulating or very undulating slopes are found in zones covering ~31.5% and ~12.4% of the total catchment surface area, respectively (CPRM, 2015). A large transition zone separates the upper and lower regions of the study basin, characterized by the sloping eastern escarpments of the Borborema granite-gneiss massif. The soil parent materials are mainly metaluminous granites (56%), orthogneisses (31%) and biotite-muscovite gneisses (8%) (Silva et al., 2015) (Fig. 1a). The main soil classes found in the study basin are Entisols (~37%), Alfisols (~18%), Ultisols (~32%) and Oxisols (~9%) (Fig. 1b).

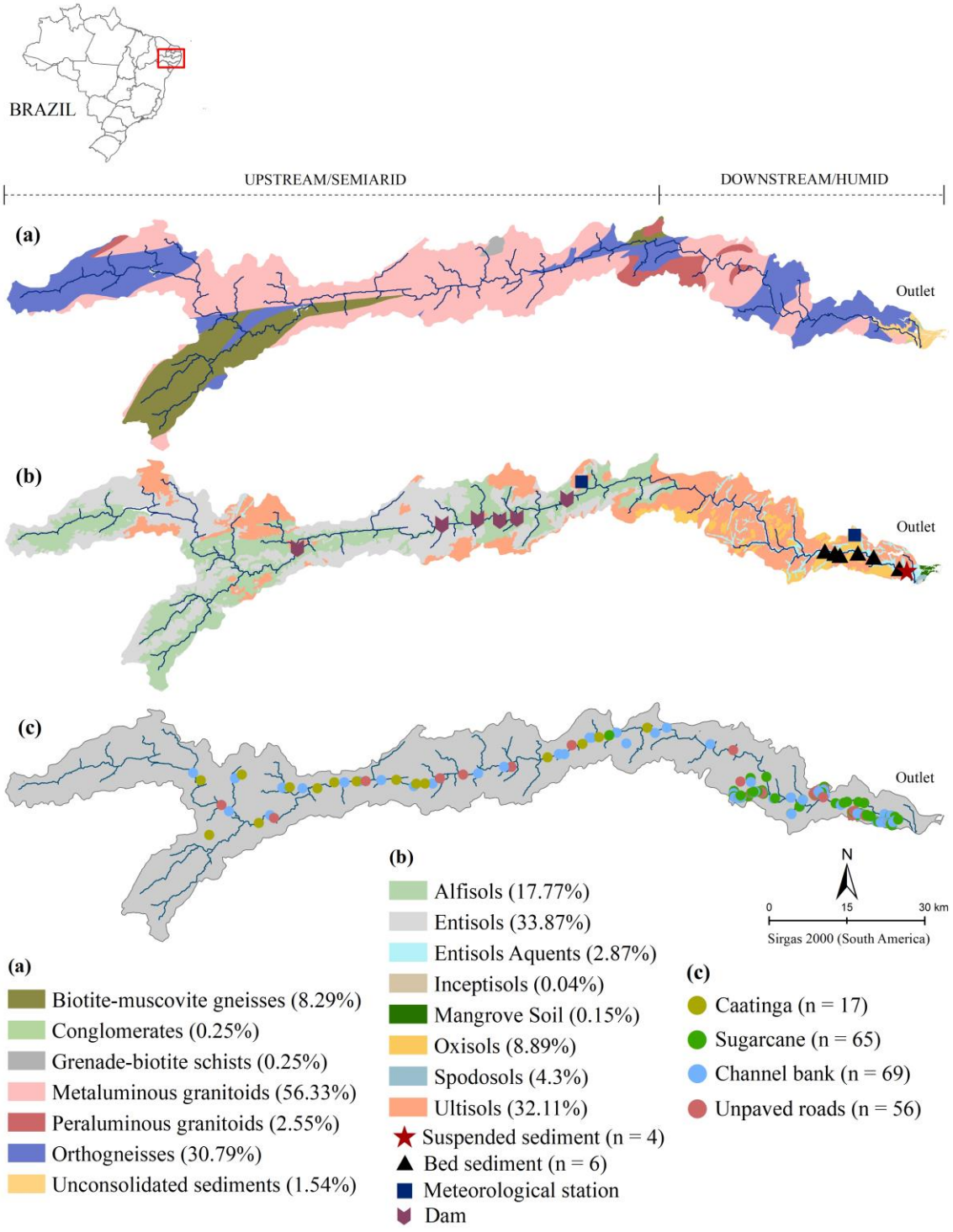

Fig. 1. Map of the Ipojuca River catchment, Northeastern Brazil, showing the distribution of the main geological (a), pedological and sampling locations for target sediment (b) and land use zones and sampling locations for potential sources (c). Dams are shown in (b).

The areas under vegetation (natural and semi-natural) and cropland cover 18% and 19% of the Ipojuca River catchment area, respectively (CONDEPE / FIDEM 2005). The *Caatinga* vegetation is found in the preserved and semi-preserved areas of the

upstream region, with typical endemic plant species resistant to arid conditions (Supplementary Figure 1). The natural vegetation in the lower catchment is the Atlantic Forest, which has been extensively degraded due to the expansion of agriculture. Nowadays, this region is characterized by small and isolated fragments of vegetation, often distant from the river network as a result of the limited preservation of riparian vegetation as well as the expansion of sugarcane (*Saccharum officinarum*) monoculture, which covers almost the entire agricultural landscape in this portion of the study basin.

2.2 Collection of source and sediment samples and sediment source classification

Soil samples (n = 207; see Fig. 1c for distribution) were collected from the main potential sources of sediment. These collection points were defined by a preliminary assessment of sediment delivery pathways using satellite images, soil, geology and slope maps, as well as field observations. Each sample (Fig. 2) was composed of 15 sub-samples collected at 0-5 cm depth for superficial sources and from the lower parts of channel bank profiles. Three source classification schemes were generated from the same sample set, based, respectively, on the distribution of land uses (1), soil classes (2), and the regional and environmental contrasts between the upper and lower portions of the study basin (3):

1. The first typology was based on land uses and covers found in the study basin. The land uses selected and the corresponding numbers of samples (Fig. 2) were: *Caatinga* – natural vegetation (n = 17); channel banks (n = 69); unpaved roads (n = 56), and; sugarcane cropland (n = 65). *Caatinga* samples represent the preserved and semi-preserved conditions found in upper semiarid areas, comprising samples collected under riparian vegetation and in areas connected to the main channel of the Ipojuca River.
2. The classification of sources based on soil classes was executed using the database of the Agroecological Zoning of Pernambuco (ZAPE) and the Brazilian System of Soil Classification (SiBCS) and by overlaying sample locations on these maps. The following soil classes were included in this classification scheme: Entisols (n = 11), Alfisols (n = 37), Ultisols (n = 76), Entisols (Aquents) (n = 57) and Oxisols (n = 26). Entisols occur mainly in the uppermost region of the study basin. The Alfisols in the study basin usually manifest a pattern of acidity from light to neutral,

sodium saturation lower than 8% at the Bt horizon, and low content of superficial organic matter. The Ultisols, mainly distributed in the downstream region, are deep, with a low natural fertility, with strong to moderate acidity, and low contents of exchangeable calcium and magnesium. The Ultisols of the upstream region are less deep, although they exhibit small chemical differences compared to the former. The Entisols (Aquents) present varied chemical characteristics as a consequence of their spatial distribution. The Oxisols are deep, with strong acidity, natural cohesion, high content of Al, and are developed mainly in the wetter areas of the basin and the upper sections of plains in the downstream region.

3. In the third classification scheme for potential sources, the same sampling set was divided into two environmentally contrasting regions: upper and lower catchment. Samples from the upstream region (n = 45) represent the combination of the dry climate with a highly spatially- and temporally-variable hydrological regime, shallow soils, intermittent and semi-intermittent fluvial regime, and the sparse occurrence of cropland. The samples (n = 162) from the downstream zone represented wet landscapes, a perennial fluvial regime, deep and well-developed soils, and extensive areas of monoculture cropland.

Target suspended sediment samples (n = 4; Fig. 1b) were collected in a cross-section located at the outlet of the main river system, by means of time-integrated samplers (Phillips et al., 2000) installed between April 2019 and February 2020, in order to capture the full range of hydrological responses (Table 1). Target bed sediment samples (n = 6) were also collected in October 2019 at the overall outlet in order to permit comparison of the source apportionment results for two target sediment types. Recovery of this material was performed by scraping the accumulated sediment, taking care not to exceed a depth of 5 cm.

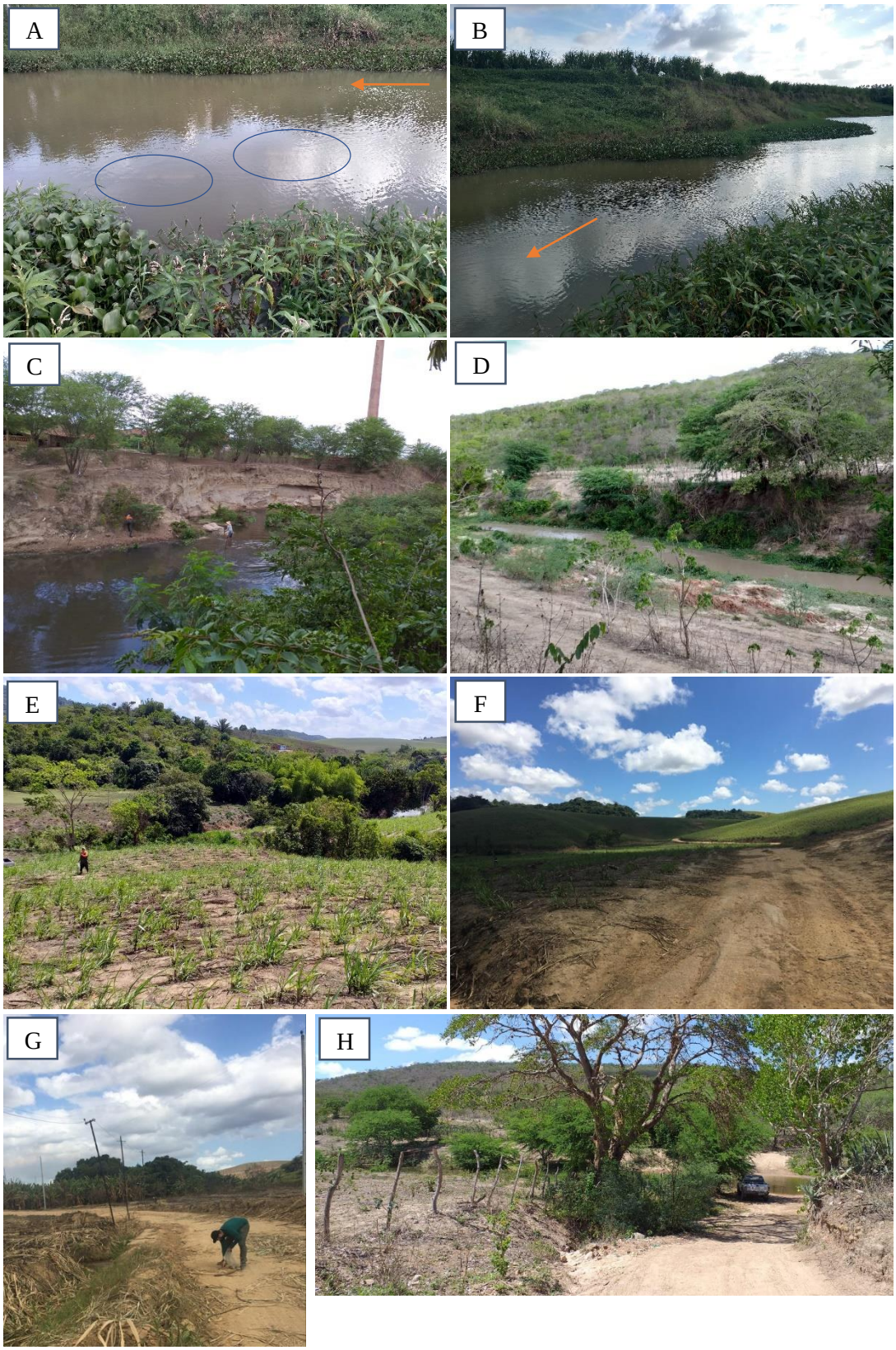

Fig. 2. Representative landscapes for potential sediment sources and sampling sites in the Ipojuca River catchment: (A) and (B) cross-sections selected downstream in the Ipojuca River for the installation of the sediment samplers during the period of higher water discharge; (C) example of

an upstream channel bank sampled; (D) channel bank and connected areas of *Caatinga* vegetation in the upstream region; (E) sugarcane in the early stages of development in downstream areas connected to the main channel; (F) unpaved roads and sugarcane crops on soils formed over typical slopes for the downstream portion of the study basin ("Mares de Morros"); (G) unpaved roads close to the downstream croplands; (H) roads with direct connectivity to the main river upstream. The orange arrows indicate the flow direction of the Ipojuca River.

Table 1. Sampling periods for target suspended sediment and the corresponding rainfall totals in the upstream and downstream portions of the Ipojuca River catchment.

Observation period*	Sample dry mass (g)	Amount of rainfall (mm) (upstream - downstream)**
04/15/19 - 05/22/19	20.4	165 – 249
05/22/19 - 06/10/19	38.9	121 – 473
09/27/19 - 12/03/19	90.0	32 – 147
12/11/19 - 02/10/20	17.2	28 – 105

* channel cross-section location: 8°24'20.90"S - 35°03'37.22"W; ** (IPA, 2019).

2.3 Sample preparation and particle size characterization

The source and target sediment samples were respectively air-dried and dried in a forced-circulation stove at 50°C. All samples were then gently disaggregated and sieved through a 2-mm mesh. Particle size distribution analysis was conducted to define the target fractions for sediment fingerprinting. Furthermore, organic matter in 2 g of each sample was burned using 20 ml H_2O_2 (25%) in a stove at 50°C for 24 to 48 h, and the dispersion of the particles was achieved by the addition of 10 ml NaOH (6%) and agitation at 130 rpm for 12 h. The absolute size distribution of particles was determined after dispersion in a liquid analyzer (Microtrac S3500), suitable for the size range 20-nm to 2-mm. In addition to the samples collected specifically for sediment fingerprinting, 25 composite samples from the superficial layer (0-20 cm) of reference soils in the study basin collected for previous work (Silva et al., 2015) were used to support the particle size characterization of the main soil classes in the area. The particle size distribution was obtained according to Gee and Or (2002).

The average diameter and D_{90} of the target suspended sediment samples from the outlet of the Ipojuca River (Supplementary Figure 2) were 12.2 μm and 24.3 μm, respectively. The silt fraction represented approximately 85% of the particle size composition of these samples. Therefore, all geochemical analyses were conducted on the <32 μm fraction, with the aim to optimize the direct comparison of the properties of the sources and target sediment.

2.4 Geochemical analysis

The contents of 20 metals were used as potential fingerprint properties: Al, Ba, Ce, Cr, Fe, La, Nd, Ni, Pb, Pr, Sc, Sm, Sn, Sr, Th, Ti, V, Y, Zn and Zr. The extraction of these metals followed the method proposed by Estévez Alvarez et al. (2001). First, 0.5 g of each source and target sediment sample was pre-digested in 10 ml of HF in a rest system for 12 h. Then, the samples were put in vessels with 5 ml of HNO_3 and 3 ml of $HClO_4$ and placed on a hot plate at 180 °C. The latter step was repeated to ensure the total dissolution of the samples. Each extract was then dissolved in 5 ml HCl and diluted in deionized water to fill a 25 ml volumetric flask. Calibration and recalibration of curves, high purity acids, reagent blanks and standard reference materials (SRM 2709 Montana Soil, National Institute of Standards and Technology, NIST, 2002) were used to ensure quality control of the analyses. The concentrations of metals in the final extracts were determined by means of inductively coupled plasma optical emission spectrometry (ICP-OES/Optima DV7000, Perkin Elmer) with a coupled cyclonic chamber system to enhance precision of the measurements. Only the total concentrations of Zr were determined by means of X-Ray fluorescence spectrometry (S8 TIGER ECO - WDXRF-1KW model). The recovery rates of the analyzed metals ranged from 48% (Zn) to 107% (Ni). More than 80% of the chemical elements showed recovery rates ranging from 80% to 100%.

2.5 Selection of tracers and apportionment of sediment sources

The successive steps for tracer selection were: (1) assessment of conservative behaviour (range test); (2) comparison of the individual sources (Kruskal-Wallis H-test), and; (3) linear discriminant analysis (forward stepwise tracer selection). Tracer conservation was assessed using a conventional range test based on the individual comparison of the minimum and maximum elemental concentrations in source material and target sediment samples. The Kruskal-Wallis H-test was used to explore and confirm individual tracer capacity for distinguishing the sediment sources ($p < 0.1$). Linear

discriminant analysis ($p < 0.1$) used the minimization of Wilk's lambda to select three final composite signatures for discriminating the sediment sources on the basis of the three classification schemes. To minimize problems associated with characterization of sources and effects of point or non-point pollution, we removed any extreme or outlier values from this fingerprinting modelling. MixSIAR (Stock and Semmens, 2016) was applied to estimate the average relative contribution of the individual sediment sources, using Markov Chain Monte Carlo (MCMC) maximum parameters: number of chains = 3; chain length = 3,000,000; burn = 2,700,000; thin = 300. The outputs from the models were rejected if a variable was above 1.01 for the Gelman-Rubin diagnosis. The averages, standard deviations, confidence intervals, and posterior correlations of source contributions were also estimated. The accuracy of the source estimates was evaluated using virtual mixtures, which were generated to compare known and predicted source contributions, using the composite signatures selected by LDA (Phillips and Gregg, 2003):

$$y = \sum_{i=1}^{n} k_i f_i \quad (1)$$

in which y is the virtual mixture, k is the result of the individual source using mixtures of target sediments, n is the number of tracers, i is the tracer used, and f is the individual source. The accuracy of the predicted source estimates was evaluated using the root mean square error (RMSE) and mean absolute error (MAE), viz.:

$$RMSE = \sqrt{\frac{\sum_{i=1}^{n}(Y_{predicted} - Y_{known})^2}{n}} \quad (2)$$

$$MAE = \frac{\sum_{i=1}^{n}|Y_{predicted} - Y_{known}|}{n} \quad (3)$$

in which $Y_{predicted}$ is the relative contribution of the sediment source predicted by the model, Y_{known} is the known relative contribution of the source to the virtual mixture and n represents the total number of sediment sources. All statistical procedures were undertaken using R software (version 3.6.1, R Core team, 2021).

3. Results

3.1 Exploratory apportionment of sediment sources

The discrimination potential of regional sources (upstream and downstream), soil classes (Ultisol, Entisol (Aquent), Oxisol, Entisol and Alfisol) and land uses (Caatinga, channel banks, sugarcane and unpaved roads) were evaluated using all geochemical

tracers by forward stepwise LDA ($p < 0.1$) (Fig. 3). This analysis showed significant overlaps between the ellipses of Ultisols and Entisols (Aquents) (Fig. 3a) as well as between those of channel banks and unpaved roads (Fig. 3c). Thus, the final sources were reclassified by merging these groups, resulting in the Ultisols + Entisols (Aquents) (Fig. 3b) and channel banks + unpaved roads (Fig. 3d). Some previous sediment fingerprinting studies have clearly pointed to improved discrimination and apportionment modelling from reclassifying initial source categories (Barthod et al., 2015; Lizaga et al., 2021). Here, in general, this merging ensured increased discriminatory power (Fig. 3b and 3d), exemplified by the rates of correctly classified samples (CCS) on the basis of soil classes improving from 66% to 90% and in the case of land uses, from 59% to 77%, respectively. The first and second linear discriminant functions accounted for much of the variance in these source groups, explaining 97% and 100% of the total variance in the soil classes (LD1 = 78%, LD2 = 19%; Fig. 3b) and land uses (LD1 = 63%, LD2 = 37%; Fig. 3d), respectively. LDA revealed high potential for differentiation between the two regional sources (Wilks' Lambda = 8; CCS = 99%).

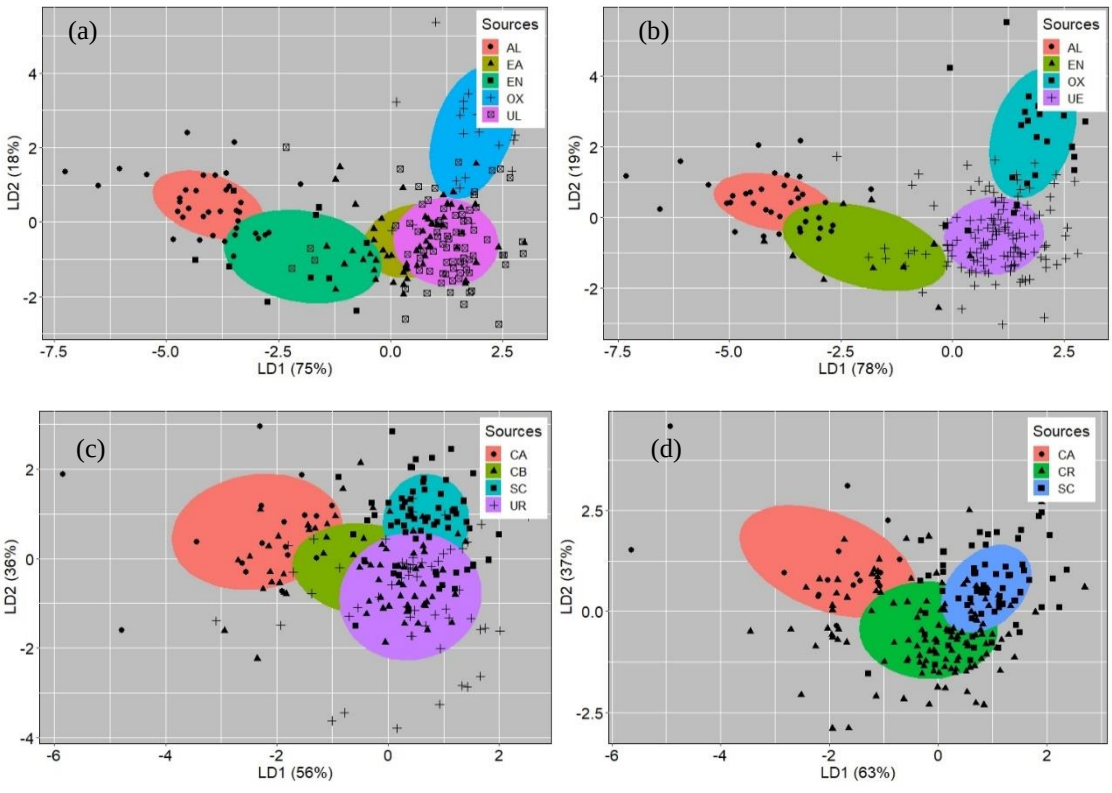

Fig. 3. Two-dimensional plots of the LDA ($p < 0.1$) of the initial (a and c) and final (b and d) source groups after reclassification of the Ipojuca River catchment sources for the samples defined as soil classes (a and b) and land use (c and d), considering all geochemical tracers. UL = Ultisol,

EA = Entisol (Aquent), OX = Oxisol, EN = Entisol, PL = Alfisol and UE = Ultisol + Entisol (Aquent); CA = Caatinga, CB = channel banks, SC = sugarcane, UR = unpaved roads, and CR = channel banks and unpaved roads.

3.2 Tracer selection

All analyzed elements in the < 32 μm fraction passed the range test (Table 2) and were therefore considered conservative during erosion and sediment transport to, and through, the river network (Supplementary Figures 3 and 4).

Table 2. Minimum and maximum values of geochemical tracer concentrations in source material and target sediment samples (suspended and bed sediments) used to assess tracer conservation.

Tracers (mg kg^{-1})	Sources (n = 207)			Suspended sediments (n = 4)			Bed sediments (n = 6)		
	Min.	Max.	Mean	Min.	Max.	Mean	Min.	Max.	Mean
Al	9240	162850	115011	103650	131200	116250	106150	137850	127200
Ba	4.1	1713.0	595.7	294.5	570.5	422.6	445.8	1040.5	773.3
Ce	44.1	329.9	137.8	129.7	138.9	134.0	88.8	138.9	121.6
Cr	5.9	123.8	38.6	7.2	48.8	37.5	35.8	55.3	41.2
Fe	4556	86600	38228	13510	45070	31932	35845	64200	46318
La	18.4	140.2	59.6	57.5	60.6	58.6	34.4	65.2	53.4
Nd	8.9	85.0	33.0	31.6	33.4	32.5	18.9	34.8	28.5
Ni	2.9	52.6	16.6	4.8	17.4	13.2	12.8	15.9	14.5
Pb	4.8	301.1	25.8	7.1	24.8	18.2	14.8	34.3	26.0
Pr	3.0	43.1	14.4	14.3	16.0	14.8	4.4	14.8	10.4
Sc	2.1	15.6	8.1	8.5	9.8	9.3	6.2	9.0	7.4
Sm	2.4	21.7	8.7	8.4	9.3	8.8	4.8	8.6	7.3
Sn	1.6	22.4	6.4	2.2	7.2	5.4	6.4	8.2	7.0
Sr	1.1	714.0	127.4	31.7	127.9	90.8	91.7	187.1	146.7
Th	11.9	111.6	34.2	26.6	29.9	28.3	20.8	35.8	29.5
Ti	266	12725	5912	1627	6225	4606	5655	7245	6657
V	6.0	181.1	73.6	18.9	87.4	63.0	59.1	80.7	71.9
Y	3.4	55.9	12.3	12.7	13.9	13.4	7.5	14.7	11.7
Zn	0.0	158.6	49.0	11.2	72.0	53.9	53.9	76.4	64.4
Zr	112.0	3441.0	643.6	135.0	376.5	215.0	270.0	961.0	536.3

Four and six elements (Table 3) failed to differentiate the samples classified on the basis of soil classes (Ce, Nd, Sm, and Zn) and regional sources (Ce, Nd, Pr, Sm, Th, and Zn). In contrast, the concentrations of all the tracers were significantly different among the sources classified on the basis of land use.

Table 3. Kruskal-Wallis H-test results for the sources classified using the geochemical tracers that passed the conservation test.

Tracers	Regions		Soil classes		Land use	
	H-value	p-value	H-value	p-value	H-value	p-value
Al	97.81	<0.01	88.29	<0.01	35.52	<0.01
Ba	52.43	<0.01	76.15	<0.01	23.38	<0.01
Ce	1.70	0.19	4.26	0.24	16.14	<0.01
Cr	11.31	<0.01	18.88	<0.01	6.41	0.04
Fe	74.69	<0.01	67.92	<0.01	34.11	<0.01
La	7.08	0.01	11.78	0.01	17.42	<0.01
Nd	0.10	0.75	0.40	0.94	12.63	<0.01
Ni	4.32	0.04	13.80	<0.01	6.31	0.04
Pb	26.82	<0.01	35.71	<0.01	14.93	<0.01
Pr	0.61	0.44	7.62	0.05	10.39	0.01
Sc	67.38	<0.01	63.89	<0.01	26.49	<0.01
Sm	1.38	0.24	1.66	0.65	12.05	<0.01
Sn	12.85	<0.01	8.43	0.04	7.67	0.02
Sr	60.94	<0.01	78.40	<0.01	24.74	<0.01
Th	0.41	0.52	18.23	<0.01	6.93	0.03
Ti	84.62	<0.01	82.95	<0.01	27.36	<0.01
V	74.54	<0.01	76.95	<0.01	23.78	<0.01
Y	67.38	<0.01	70.44	<0.01	38.06	<0.01
Zn	0.54	0.46	2.69	0.44	4.69	0.10
Zr	25.98	<0.01	36.09	<0.01	15.39	<0.01

The LDA forward stepwise analysis selected sets of eight tracers for the regional sources (Al, Sr, Y, Ti, Pb, La, Fe, and Zr), ten for the soil classes (Al, Ba, Ni, Ti, La, Pr, Sr, Zr, Th, and Sc) and six for the land use sources (Al, Ce, Ti, V, Pb, and Sr) (Table 4). These sets explained 75% of the differences between regional sources, 81% in the case of the soil classes, and 45% for the land uses, as per Wilks' Lambda cumulative (LW),

and were able to correctly classify 97% of the regional samples, 86% of the soil class samples and 72% of the land use samples. Individual discrimination error rates ranged from 4% to 17% (regional sources), 20% to 37% (soil classes), and 37% to 42% (land uses) (Supplementary Figures 5 and 6). Only Al, Ti and Sr were selected in all three approaches, highlighting mainly the high individual discriminatory power of Al and Ti for soil classes and regional sources.

Table 4. Final composite signatures selected by linear discriminant analysis and corresponding parameters for the three classifications of sediment sources in the Ipojuca River catchment.

Tracers	Wilks' lambda	F-value	p-value	IER (%)	CER (%)
Regions					
Al	0.40	311.82	<0.01	4.3	4.3
Sr	0.33	208.01	<0.01	8.1	3.3
Y	0.31	153.50	<0.01	11.8	3.3
Ti	0.29	125.92	<0.01	15.3	1.9
Pb	0.28	105.49	0.01	16.3	1.9
La	0.27	91.29	0.01	16.9	1.9
Fe	0.26	80.23	0.04	15.9	1.9
Zr	0.25	72.68	0.02	17.2	2.9
Soil classes					
Al	0.46	80.64	<0.01	20.7	20.7
Ba	0.35	46.97	<0.01	33.3	21.7
Ni	0.30	34.29	<0.01	34.2	20.7
Ti	0.28	27.00	<0.01	22.7	18.8
La	0.25	23.83	<0.01	35.7	19.3
Pr	0.22	21.87	<0.01	35.7	15.4
Sr	0.21	19.44	0.01	35.7	15.4
Zr	0.20	17.59	0.02	34.3	16.4
Th	0.19	15.99	0.06	35.7	15.4
Sc	0.19	14.68	0.09	37.1	13.5
Land uses					
Al	0.78	28.31	<0.01	42.0	42.0
Ce	0.72	18.40	<0.01	37.1	40.1
Ti	0.66	15.43	<0.01	40.0	35.7
V	0.61	14.34	<0.01	39.6	31.8
Pb	0.57	12.84	<0.01	39.6	31.4
Sr	0.55	11.67	0.01	40.0	28.0

IER = individual error rate; CER = cumulative error rate.

3.3 Estimated sediment source contributions

Fig. 4 presents source type contributions to SS and BS samples estimated by MixSIAR modelling. The Oxisols and sugarcane cultivation were the dominant sources in the downstream region. For SS, the proportional contributions followed the order: (a) regional, Downstream > Upstream; (b) soil classes, Oxisols > Ultisols + Entisols (Aquents) > Entisols > Alfisols; (c) land uses, sugarcane > channel bank + unpaved roads > Caatinga. For BS, the results were similar, except for the relative importance of soil classes: Entisols > Oxisols > Ultisols + Entisols > Alfisols.

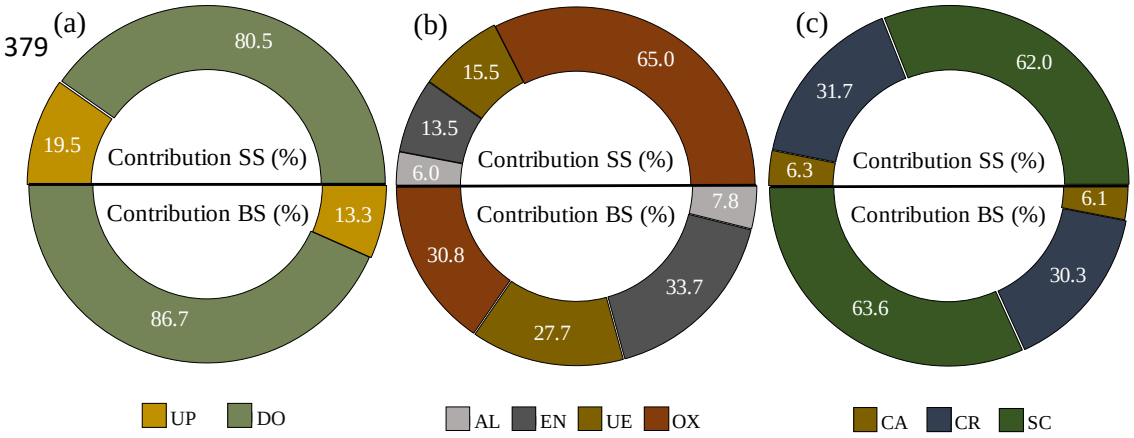

Fig. 4. Average relative contributions of suspended sediment (SS) and bed sediment (BS) sources classified on the basis of regions (a), soil classes (b) and land use (c). UP = Upstream and DO = Downstream; AL = Alfisol, EN = Entisol, OX = Oxisol and UE = Ultisol + Entisol (Aquent); CA = Caatinga, CR = channel bank + unpaved road, SC = sugarcane.

The source estimates predicted by MixSIAR were similar to the known proportions used to generate virtual mixtures, suggesting acceptable accuracy (Table 5). The RMSEs and MAEs ranged from 0.1-6.0% and 0.1-4.9%, respectively, and their respective overall means were 3.6% and 3.3%. Correlations among the estimated posterior contributions were generally weak; -0.30 for soil classes and -0.42 for land uses (Supplementary Figures 7, 8, and 9). However, strong negative correlations were observed between the contributions of Ultisol + Entisol (Aquent) and Oxisol (-0.71) and sugarcane, channel banks + unpaved roads (-0.95) and upstream and downstream (-1.00).

Table 5. Comparison of the mean known (MC) and predicted (MP) contributions of the different sources of target suspended sediment (SS) and bed sediment (BS) samples using virtual mixtures and statistical tests for the accuracy of MixSIAR outputs.

	Sources	Target sediment	MC (%)	SD (%)	MP (%)	RMSE	MAE
Regions	Upstream	SS	19.5	10.2	24.4	4.9	4.9
	Downstream		80.5	10.2	75.6		
	Upstream	BS	13.3	6.3	13.4	0.1	0.1
	Downstream		86.7	6.3	86.6		
Soil classes	Alfisol	SS	6.0	5.7	11.0	5.3	4.9
	Entisol		13.5	7.0	11.4		
	Oxisol		65.0	9.3	57.2		
	Ultisol-Entisol (Aquent)		15.5	8.6	20.4		
	Alfisol	BS	7.8	6.0	16.3	6.0	4.7
	Entisol		33.7	9.3	25.3		
	Oxisol		30.8	9.1	31.8		
	Ultisol-Entisol (Aquent)		27.7	11.3	26.6		
Land use	Caatinga	SS	6.2	6.0	7.5	2.5	2.3
	Channel bank + unpaved roads		31.7	17.5	34.0		
	Sugarcane		62.0	17.7	58.5		
	Caatinga	BS	6.1	4.3	6.8	2.8	2.5
	Channel bank + unpaved roads		30.3	13.6	33.4		
	Sugarcane		63.6	13.4	59.8		

UP = Upstream and DO = Downstream; AL = Alfisol, EN = Entisol, OX = Oxisol and UE = Ultisol + Entisol (Aquent); CA = Caatinga, CR = channel bank + unpaved road, SC = sugarcane; standard deviation (SD); root mean squared error (RMSE) and mean absolute error (MAE).

4. Discussion

4.1 Tracer conservation and sediment source discrimination

All tracers passed the range test using the <32 μm fraction of source and target sediment samples collected in the Ipojuca River catchment. Nevertheless, it is important to bear in mind the limitations of such tests (Batista et al., 2019; Collins et al., 2020; Ramon et al., 2020). Elements with higher enrichment potential linked to anthropogenic activities in the study basin, such as Ca, Mg, Mn, P, and K, were disregarded in this study. A high degree of anthropogenic enrichment of Pb, Ni, and Zn in downstream river sediments has been reported for the study river by previous work (Silva et al., 2017). In general, however, different trace elements exhibit limited enrichment in sediments at the downstream sites in the study area (Silva et al., 2017; Silva et al., 2018b; Nascimento et al., 2019).

Although the Ultisols and Entisols (Aquents) generally show distinct geochemical signatures, the surface samples of these soil classes expressed strong similarity in the Ipojuca River catchment (Fig. 3b). Ultisols and Entisols (Aquents) are distributed in adjacent areas of the east-central portion of the study basin (Fig. 1b), indicating that these soils may be derived from geochemically similar parent materials. In addition, based on field observations, distribution maps (Fig. 1), and the particle size of these river basin sources (Supplementary Table 1), the Entisols (Aquents), located on the lower elevations of the local geomorphological interfluves, may be the receptors of material eroded in the steeper neighbouring areas represented by Ultisols (Fig. 1b). As a result, it is possible that some samples collected in areas represented by the Entisols (Aquents) may represent mixtures. Furthermore, the similarity between channel banks and unpaved roads highlights the lack of substantial differences in the subsurface geochemical signatures of the soils where these sources are found. Overall, unpaved roads represent subsurface sections that have been exposed at the foot of many steeper slope reliefs in the study basin, whilst channel banks have been reported to exhibit similar signatures to other nearby sources in some river catchments (Vale et al., 2020).

Only Al, Ti, and Sr were selected in the final composite signatures for discriminating the catchment sediment sources using all three source classifications, reflecting the high KW H-values for source discrimination by these individual tracers. Aluminum and Ti can express key differences in association with the development stage of soils. Al, for example, is widely used in indices of chemical weathering, such as the CIA method (Nesbitt and Young, 1982). The tendency here is that higher Al and Ti

contents are observed in more weathered and developed superficial horizons due to the high strength and low mobility of these elements (Koiter et al., 2013; Smith et al., 2018). The mean Al and Ti concentrations measured in our samples (Table 6) distinguished upstream (73.5 g kg^{-1} and 3550.5 mg kg^{-1}) from downstream sources (126.5 g kg^{-1} and 6567.9 mg kg^{-1}) and Alfisols (72. 7 g kg^{-1} and 3427.4 mg kg^{-1}) and Entisols (99.7 g kg^{-1} and 4901.3 mg kg^{-1}) from Ultisol-Entisols (Aquent) (127.2 g kg^{-1} and 6662.6 mg kg^{-1}) and Oxisols (119.2 g kg^{-1} and 6035.3 mg kg^{-1}). However, this was not the case for the land use sources when considering sugarcane and Caatinga as surface sources and channel banks + unpaved roads as subsurface sources: sugarcane (118.6 g kg^{-1} and 5759.1 mg kg^{-1}), Caatinga (71.1 g kg^{-1} and 3130.9 mg kg^{-1}) and channel banks + unpaved roads (119.0 g kg^{-1} and 5268.7 mg kg^{-1}). With respect to Al, this is because channel banks + unpaved roads represent both the more developed soils (Ultisol-Entisol (Aquent) and Oxisol) downstream and the less developed soils (Entisol and Alfisol) upstream. Another factor reducing source discrimination is the disturbance and incorporation of the surface and subsurface soil layers during sugarcane management in the study catchment. Iron, selected only in the composite signature for discriminating regional sources, was expected to exhibit similar discriminant patterns as Al and Ti for the soil classes because of the potential for oxide accumulation in the more developed soils found downstream. The average concentrations of Ba, Sr and Zr ensured discrimination between Ultisol + Entisols (Aquent) (525.6 mg kg^{-1}, 108.6 mg kg^{-1} and 630.3 mg kg^{-1}) and Oxisols (277.8 mg kg^{-1}, 71.3 mg kg^{-1} and 390.5 mg kg^{-1}); Sr and Ce improved discrimination between sugarcane (118.0 mg kg^{-1} and 105.3 mg kg^{-1}) and channel banks + unpaved roads (148.1 mg kg^{-1} and 124.9 mg kg^{-1}), although this benefit for source discrimination was not so pronounced in the case of soil classes (Supplementary Tables 3 and 4).

Table 6. Mean concentrations and coefficients of variation (CV) of the tracers selected in the final composite signatures for discriminating the sediment sources in the study basin using all three classification schemes.

Sources/Sediment		Parameters	Al (g kg^{-1})	Sr (mg kg^{-1})	Ti (mg kg^{-1})
Regional	Upstream	Mean	73.5	210.9	3550.5
		CV	17.0%	49.0%	31.0%
	Downstream	Mean	126.5	104.2	6567.9
		CV	15.0%	47.9%	25.0%
Soil classes	Ultisol-Entisol (Aquent)	Mean	127.2	108.6	6662.6
		CV	14.0%	46.7%	24.9%
	Oxisol	Mean	119.3	71.3	6035.3
		CV	22.6%	33.8%	29.0%

	Entisol	Mean	99.7	206.0	4901.3
		CV	32.2%	36.6%	28.4%
	Alfisol	Mean	72.7	210.9	3427.4
		CV	14.0%	50.4%	28.3%
Land use	Caatinga	Mean	71.2	230.2	3130.9
		CV	12.8%	60.0%	24.9%
	Sugarcane	Mean	118.6	105.3	5759.1
		CV	18.8%	49.0%	27.48%
	Channel Banks + Unpaved roads	Mean	119.0	124.9	5268.7
		CV	23.2%	55.0%	37.37%
Suspended sediments		Mean	116,2	90.8	4605.8
		CV	10.3%	45.9%	44.5%
Bed sediments		Mean	127.2	146.7	6656.6
		CV	9.0%	24.9%	9.6%

Additional data for the mean concentrations and coefficients of variation (CV) of the LDA-selected elements can be found in supplementary Tables 1, 2, 3, 4 and 5.

The regional and soil class sources had the lowest discrimination errors reflecting the influence of pedogenetic processes on tracer signatures. Other studies have reported successful discrimination of soil classes in large catchments in Brazil (Le Gall et al., 2017; Batista et al., 2019). The higher discrimination errors obtained when the sources were classified on the basis of land use reconfirmed the difficulty of geochemically differentiating these sources in large heterogeneous basins (Pulley et al., 2015; Pulley et al., 2017). For example, the overall average coefficient of variation (CV) for individual tracers for the sources classified on the basis of land use (42%) was slightly higher than for regional sources (40%) and soil classes (36%). This same trend was also followed by the average CVs of the common tracers selected in the composite signatures for discriminating sources using all three classification schemes (Al, Ti, and Sr): land use (34%) > regional sources (31%) > classes (30%). Caatinga (mean CV = 52%) and channel banks + unpaved roads (mean CV = 39%) contributed strongly to the variations in the case of sources classified by land use, with the highest value (137%) measured for Pb concentrations in Caatinga. The distribution of the channel banks + unpaved roads samples in the basin (Fig. 1c) may explain this scenario, since about 30% and 70% of these samples, respectively, were collected along the upper and central parts of the study basin (i.e., representing very different lithological, pedological and climatic contexts). Despite this pattern of intra-source variability and the corresponding higher LDA errors, all the RMSE and MAE estimates for the predicted source proportions using the land use classification were acceptably low and, in fact, similar to the corresponding errors calculated when the sources were classified on the basis of regional sources or soil classes, indicating acceptable confidence in all of the predicted source proportions.

4.2 Contribution patterns of different source types

Most (SS = 81% and BS = 87%) of the sampled sediments transported in the Ipojuca River at the outlet were predicted to originate from sources located in the downstream region of the study catchment. This distribution pattern reflects several contrasting hydro-climatic and environmental conditions. The downstream areas comprise environments characterized by a humid climate (average annual rainfall of about 2400 mm $year^{-1}$), whereas the upstream portion is typically represented by a semiarid climate (i.e., average rainfall of about 600 mm $year^{-1}$). Accordingly, rainfall erosivity is threefold higher downstream than in the upstream region of the study basin (Cantalice et al., 2009). The small contribution of the upstream sources (SS and BS < 20%) is likely to have been reduced by the dams built upstream of the main channel. These structures can significantly decrease longitudinal connectivity, which means longer sediment trapping and residence times in that portion of the study catchment and a lower transfer rate to the downstream portion (Kitamura et al., 2014; Silva et al., 2015; Batista et al., 2019). Our results indicate, however, that the dams did not result in total sedimentary disconnection during the observation period. As Cucchiaro et al. (2019) underlined, dams can be ineffective in the case of large flows, continuing to release trapped sediments.

Soils located in the downstream part of the study catchment (Oxisol, Ultisol + Entisol (Aquent)) were the main sediment sources, contributing an average of 80% and 58% of the target suspended and bed sediment samples, respectively. Entisols and Alfisols in the western (upstream) portion of the study basin were predicted to supply low contributions to the sampled target sediments. Our sediment fingerprinting estimates suggested high contributions (60%) from Oxisols to target suspended sediment samples; three times higher than the corresponding contributions from the other soil classes. Although they are deep soils with greater infiltration capacity and cover only about 9% of the study basin, the Oxisols are mainly distributed in the downstream region and in areas closer to the main river channels (represented in yellow in Fig. 1b). This distribution enhances hydrological and sedimentological connectivity with the overall outlet sampling site for the target sediment samples. In contrast, the Ultisols comprise 32% of the study catchment but are often found in areas with lower slope-to-channel connectivity than the Oxisols. The low contribution of the Ultisol + Entisol (Aquent) soil combination may be associated with the fine texture in the surface layer of the Ultisols (Supplementary Table 1) and the limited spatial coverage of the study area by the Entisols (Aquents) (<1.5%).

Sediment source apportionment based on the land use classification of potential sources also underlined the importance of the downstream region of the study area. Sugarcane contributed 62% and 64% of the target suspended and bed sediment sampled. In contrast, Caatinga contributed only 6% to both types of target sediment.

The sugarcane contribution to sediment samples shows the importance of the surface erosion processes in the study catchment. Its protective vegetation cover during the more advanced development stages buffers the soil against erosion processes (Bezerra and Cantalice, 2006; Amorim et al., 2021), but the post-harvest period and the initial development stages are likely associated with the high soil erosion in this land use. Our results suggested that channel banks plus unpaved roads are the second most important sediment source classified by land use. This reflects the lack of riparian vegetation along the Ipojuca River in the case of the channel banks. High unpaved road contributions have been observed in other watersheds in Brazil, but these are typically relatively low compared to other sources, mainly due to the small surface areas of these sources in the catchments investigated (Tiecher et al., 2018; Ramon et al., 2020; Amorim et al. 2021).

Sediment source apportionment based on soil classes alone led to contrasting results for SS and BS. The Oxisols and Entisols are mainly responsible for this pattern. These results may reflect a legacy from accumulated bed sediment-associated metal pollution in the river in in the downstream region, since the average metal concentrations were higher than those observed in SS, except for Pr and Sc (Supplementary Figures 2 and 3).

Overall, the Oxisols under sugarcane represent the most important sediment source. However, the source apportionment estimates are scale-dependent (Batista et al., 2019; Koiter et al., 2013), meaning that the predicted source contributions would most likely differ for target sediment sampling sites located further upstream. Minimizing errors associated with the classification of sediment sources on the basis of land use is a challenge for future studies in the large river catchments typical of Brazil. Here, there is a need to explore the utility of additional and novel tracers. In this regard, previous work in Brazil has illustrated the utility of optical property composite signatures (Amorim et al., 2021) and total P concentrations and their fractionation (Tiecher et al., 2019). The latter could be useful for our study basin, since in the downstream part of the catchment, topsoil layers under tillage tend to have higher P contents, compared with channel banks and unpaved roads, due to the use of phosphate fertilizers. This potential to use P-based tracers is enhanced by the ability of clay minerals, typical of the more developed soils in

559 the downstream region of our study basin, to fix P in their structures, generating
560 potentially useful signatures to assist sediment source discrimination. Other possibilities
561 are to test environmental DNA to characterize the dominant plant communities found in
562 soils under Caatinga and sugarcane (Evrard et al., 2019; Foucher et al., 2020a), the
563 composition of organic matter in soils from different land uses (Laceby et al., 2016;
564 Foucher et al., 2020b) and the compound specific stable isotopes (Upadhayay et al. 2017).

565 **Conclusions**

566 Application of different classifications of sediment sources has enhanced the level
567 of detail on sediment source patterns in the study basin. The more detailed information
568 generated using more than one source area classification scheme better supports the
569 targeting of sediment management.

570 Future research could use sedimentary deposits for the temporal reconstruction of
571 sediment source patterns in the semiarid region of the basin. Erosion control in
572 downstream landscapes with Oxisols under sugarcane cultivation should be a priority for
573 reducing the delivery of sediments and associated contaminants towards the estuarine and
574 mangrove environments. Our study herein supports future sediment source fingerprinting
575 studies in areas crossing semiarid and coastal environments under threat from excessive
576 erosion and sediment delivery.

577 **Acknowledgements**

578 Y.J.A.B. Silva is grateful to the National Council for Scientific and Technological
579 Development – CNPq for research productivity scholarships (Process Number:
580 303221/2019-4). The contribution to this manuscript by ALC was funded by UKRI-
581 BBSRC (UK Research and Innovation-Biotechnology and Biological Sciences Research
582 Council) grant award BBS/E/C/000I0330. This study was financed in part by the
583 Coordenação de Aperfeiçoamento de Pessoal de Nível Superior - Brasil (CAPES) -
584 Finance Code 001.

585 **References**

586

587 Agência Condepe/Fidem, 2005. Rio Ipojuca, Recife. Série Bacias Hidrográficas de
588 Pernambuco, 1.

589

590 Amorim, F.F., da Silva, Y.J.A.B., Nascimento, R.C., da Silva, Y.J.A.B., Tiecher, T., do
591 Nascimento, C.W.A., Minella, J.P.G., Zhang, Y., Ram, H.U., Pulley, S. Collins, A.L.,

2021. Sediment source apportionment using optical property composite signatures in a rural catchment, Brazil. Catena. 202, 105208.

Anache, J.A., Wendland, E.C., Oliveira, P.T., Flanagan, D.C., Nearing, M.A., 2017. Runoff and soil erosion plot-scale studies under natural rainfall: A meta-analysis of the Brazilian experience. Catena. 152, 29-39.

Barthod, L.R., Liu, K., Lobb, D. A., Owens, P.N., Martínez-Carreras, N., Koiter, A.J., Petticrew, E.L., Mccullough, G.K., Liu, C., Gaspar, L., 2015. Selecting color-based tracers and classifying sediment sources in the assessment of sediment dynamics using sediment source fingerprinting. J. Environ. Qual. 44(5), 1605-1616.

Batista, P.V., Laceby, J.P., Silva, M.L., Tassinari, D., Bispo, D.F., Curi, N., Davies, J., Quinton, J.N., 2019. Using pedological knowledge to improve sediment source apportionment in tropical environments. J. Soils Sediments. 19(9), 3274-3289.

Bezerra, S.A., Cantalice, J.R.B., 2006. Erosão entre sulcos em diferentes condições de cobertura do solo, sob cultivo da cana-de-açúcar. Rev. Bras. Cienc. Solo. 30(3), 565-573.

Cantalice, J.R.B., Bezerra, S.A., Figueira, S.B., Inácio, E.D.S.B., de Oliveira Silva, M.D.R., 2009. Linhas isoerosivas do estado de Pernambuco-1ª aproximação. Rev. Caatinga. 22(2), 75-80.

Collins, A.L., Walling, D.E., Webb, L., King, P. 2010. Apportioning catchment scale sediment sources using a modified composite fingerprinting technique incorporating property weightings and prior information. Geoderma. 155(3-4), 249-261.

Collins, A.L., Pulley, S., Foster, I.D.L., Gellis, A., Porto, P. and Horowitz, A.J. 2017. Sediment source fingerprinting as an aid to catchment management: a review of the current state of knowledge and a methodological decision-tree for end-users. J. Environ. Qual. 194, 86-108.

Collins, A.L., Blackwell, M., Boeckx, P., Chivers, C.A., Emelko, M., Evrard, O., Foster, I., Gellis, A., Gholami, H., Granger, S., Harris, P., Horowitz, A.J., Laceby, J.P., Martinez-carreras, N., Minella, J., Mol, L., Nosrati, K., Pulley, S., Silins, U., Silva, Y.J.A.B., Stone, M., Tiecher, T., Upadhayay, H.R., Zhang, Y., 2020. Sediment source fingerprinting: benchmarking recent outputs, remaining challenges and emerging themes. J. Soils Sediments. 20(12), 4160-4193.

Cucchiaro, S., Cazorzi, F., Marchi, L., Crema, S., Beinat, A., Cavalli, M., 2019. Multi-temporal analysis of the role of check dams in a debris-flow channel: Linking structural and functional connectivity. Geomorphology. 345, 106844.

Didoné, E.J., Minella, J.P.G., Merten, G.H., 2015. Quantifying soil erosion and sediment yield in a catchment in southern Brazil and implications for land conservation. J. Soils Sediments. 15(11), 2334-2346.

Estévez Alvarez, J., Montero, A., Jiménez, N., Muñiz, U., Padilla, A., Molina, R., Quicute de Vera, S., 2001. Nuclear and related analytical methods applied to the determination of

Cr, Ni, Cu, Zn, Cd and Pb in a red ferralitic soil and Sorghum samples. J. Radioanal. Nucl. Ch. 247(3), 479-486.

Evrard, O., Poulenard, J., Némery, J., Ayrault, S., Gratiot, N., Duvert, C., Prat, C., Lefèvre, I., Bonté, P., Esteves, M., 2013. Tracing sediment sources in a tropical highland catchment of central Mexico by using conventional and alternative fingerprinting methods. Hydrol. Process. 27(6), 911-922.

Evrard, O., Laceby, J.P., Ficetola, G.F., Gielly, L., Huon, S., Lefevre, I., Onda, Y., Poulenard, J., 2019. Environmental DNA provides information on sediment sources: a study in catchments affected by Fukushima radioactive fallout. Science of The Total Environment, 665, 873-881.

Foucher, A., Evrard, O., Ficetola, G.F., Gielly, L., Poulain, J., Giguet-Covex, C., Laceby, J.P., Salvador-Blanes, S., Cerdan, O., Poulenard, J., 2020a. Persistence of environmental DNA in cultivated soils: implication of this memory effect for reconstructing the dynamics of land use and cover changes. Sci Rep. 10(1), 1-12.

Foucher, A., Evrard, O., Huon, S., Curie, F., Lefèvre, I., Vaury, V., Cerdan, O., Vandromme, R., Salvador-Blanes, S., 2020b. Regional trends in eutrophication across the Loire river basin during the 20th century based on multi-proxy paleolimnological reconstructions. Agric. Ecosyst. Environ. 301, 107065.

Gee, G.W., Or, D., 2002. Particle size analysis. In Dane JH, Topp GC (4 ed) Methods of soil analysis: Physical methods. Soil Sci Soc Am J. 255–293.

Haddadchi A., Ryder D.S., Evrard O., Olley J., 2013. Sediment fingerprinting in fluvial systems: review of tracers, sediment sources and mixing models. Int J Sediment Res. 28, 560-578

IBGE - instituto brasileiro de geografia e estatística, 2015. Indicadores de desenvolvimento sustentável: Brasil., Coordenação de Recursos Naturais e Estudos Ambientais [e] Coordenação de Geografia, Rio de Janeiro. – (Estudos e pesquisas. Informação geográfica. 352p.

IPA - Instituto agronômico de Pernambuco, 2019. http://www.ipa.br/indice_pluv.php (accessed 12 March 2020)

Kitamura, A., Yamaguchi, M., Kurikami, H., Yui, M., Onishi, Y., 2014. Predicting sediment and cesium-137 discharge from catchments in eastern Fukushima. Anthropocene. 5, 22-31.

Koiter, A.J., Lobb, D.A., Owens, P.N., Petticrew, E.L., Tiessen, K.H., Li, S., 2013. Investigating the role of connectivity and scale in assessing the sources of sediment in an agricultural watershed in the Canadian prairies using sediment source fingerprinting. J. Soils Sediments. 13(10), 1676-1691.

Laceby, J.P., Huon, S., Onda, Y., Vaury, V., Evrard, O., 2016. Do forests represent a long-term source of contaminated particulate matter in the Fukushima Prefecture?. J. Environ. Manage. 183, 742-753.

Le Gall, M., Evrard, O., Foucher, A., Laceby, J.P., Salvador-Blanes, S., Thil, F., Dapoigny, A., Lefèvre, I., Cerdan, O., Ayrault, S., 2016. Quantifying sediment sources in a lowland agricultural catchment pond using 137Cs activities and radiogenic 87Sr/86Sr ratios. Sci. Total Environ. 566, 968-980.

Le Gall, M., Evrard, O., Dapoigny, A., Tiecher, T., Zafar, M., Minella, J.P.G., Laceby, J.P., Ayrault, S., 2017. Tracing sediment sources in a subtropical agricultural catchment of Southern Brazil cultivated with conventional and conservation farming practices. Land Degrad. Dev. 28(4), 1426-1436.

Lepage, H., Laceby, J. P., Bonté, P., Joron, J. L., Onda, Y., Lefèvre, I., Ayrault, S., Evrard, O., 2016. Investigating the source of radiocesium contaminated sediment in two Fukushima coastal catchments with sediment tracing techniques. Anthropocene. 13, 57-68.

Lima Barros, A.M., do Carmo Sobral M., Gunkel, G., 2013. Modelling of point and diffuse pollution: application of the Moneris model in the Ipojuca river basin, Pernambuco State, Brazil. Wat. Sci. Tech. 68(2), 357–365.

Lizaga, I., Bodé, S., Gaspar, L., Latorre, B., Boeckx, P., Navas, A., 2021. Legacy of historic land cover changes on sediment provenance tracked with isotopic tracers in a Mediterranean agroforestry catchment. J. Environ. Manage. 288, 112291.

Molisani, M.M., Kjerfve, B., Silva, A.P., Lacerda, L.D., 2006. Water discharge and sediment load to Sepetiba Bay from an anthropogenically-altered drainage basin, SE Brazil. J. Hydrol. 331(3-4), 425-433.

Nascimento, R.C., da Silva, Y.J.A.B., do Nascimento, C.W.A., da Silva, Y.J.A.B., da Silva, R.J.A.B., Collins, A.L., 2019. Thorium content in soil, water and sediment samples and fluvial sediment-associated transport in a catchment system with a semiarid-coastal interface, Brazil. Environ. Sci. Pollut. R. 26(32), 33532-33540.

NIST - National Institute of Standards and Technology, 2002. Standard Reference Materials -SRM 2709, 2710 and 2711.

Nesbitt, H., Young, G.M., 1982. Early Proterozoic climates and plate motions inferred from major element chemistry of lutites. Nature. 299(5885), 715-717.

Phillips, J.M., Russell, M.A., Walling, D.E., 2000. Time-integrated sampling of fluvial suspended sediment: a simple methodology for small catchments. Hydrol. Process. 14(14), 2589-2602.

Phillips, D.L., Gregg, J.W., 2003. Source partitioning using stable isotopes: coping with too many sources. Oecologia. 136(2), 261-269.

Pulley, S., Foster, I., Antunes, P., 2015. The uncertainties associated with sediment fingerprinting suspended and recently deposited fluvial sediment in the Nene river basin. Geomorphology. 228, 303-319.

Pulley, S., Foster, I., Collins, A.L., 2017. The impact of catchment source group classification on the accuracy of sediment fingerprinting outputs. J. Environ. Manage. 194, 16-26.

Ramon, R., Evrard, O., Laceby, J.P., Caner, L., Inda, A.V., De Barros, C.A., Minella, J. P., Tiecher, T., 2020. Combining spectroscopy and magnetism with geochemical tracers to improve the discrimination of sediment sources in a homogeneous subtropical catchment. Catena. 195, 104800.

Regionalização de vazões nas bacias hidrográficas brasileiras: estudo da vazão de 95% de permanência da sub-bacia 39. Bacias dos rios Capibaribe, Ipojuca, Una, Goiana, Mundaú, Paraíba, Coruripe, Pratagi, Sirinhaém, São Miguel, Camaragibe, Abiaí, Gramame e Manguaba. / CPRM – Serviço Geológico do Brasil; execução técnica e autoria de Keyla Almeida dos Santos. – Recife: CPRM, 2015.

Silva, Y.J.A.B., Cantalice, J.R.B., Singh, V.P., do Nascimento, C.W.A., Piscoya, V. C., Guerra, S.M., 2015. Trace element fluxes in sediments of an environmentally impacted river from a coastal zone of Brazil. Environ. Sci. Pollut. R. 22(19), 14755-14766.

Silva, Y.J.A.B., Cantalice, J.R.B., do Nascimento, C.W.A., Singh, V.P., da Silva, Y.J.A.B., Silva, C.M.C.A.C., Silva, M.O., Guerra, S.M., 2017. Bedload as an indicator of heavy metal contamination in a Brazilian anthropized watershed. Catena. 153, 106-113.

Silva, E.M., Medeiros, P., Araújo, J.C.D., 2018a. Applicability of fingerprinting for identification of sediment sources in a mesoscale semiarid catchment. Eng. Agric. 38, 553-562.

Silva, Y.J.A.B., do Nascimento, C.W.A, da Silva Y.J.A.B., Amorim, F.F., Cantalice, J.R.B., Singh, V.P., Collins, A.L., 2018b. Bed and suspended sediment-associated rare earth element concentrations and fluxes in a polluted Brazilian river system. Environ. Sci. Pollut. R. 25(34), 34426–34437.

Silva, Y.J.A.B., Nascimento, C.W.A., Biondi, C.M., Van Straaten, P., Silva, Y.J.A.B., Souza Júnior, V.S., Araújo, J.C.T., Alcantara, V.C., Silva, F.L., Silva, R.J.A.B., 2020. Concentrations of major and trace elements in soil profiles developed over granites across a climosequence in northeastern Brazil. Catena. 193, 104641.

Smith, H.G., Karam, D.S., Lennard, A.T., 2018. Evaluating tracer selection for catchment sediment fingerprinting. J. Soils Sediments. 18(9), 3005-3019.

Stock, B.C., Semmens, B.X., 2016. MixSIAR, G.U.I. User Manual. Version 3, 1.

Strauch, M., Lima, J.E., Volk, M., Lorz, C., Makeschin, F., 2013. The impact of Best Management Practices on simulated streamflow and sediment load in a Central Brazilian catchment. J. Environ. Manage. 127, S24-S36.

Tiecher, T., Minella, J.P.G., Evrard, O., Caner, L., Merten, G.H., Capoane, V., Didoné, E. J.; Dos Santos, D.R., 2018. Fingerprinting sediment sources in a large agricultural

790 catchment under no-tillage in Southern Brazil (Conceição River). Land Degrad. Dev.
791 29(4), 939-951.
792
793 Tiecher, T., Ramon, R., Laceby, J.P., Evrard, O., Minella, J.P.G., 2019. Potential of
794 phosphorus fractions to trace sediment sources in a rural catchment of Southern Brazil:
795 comparison with the conventional approach based on elemental geochemistry. Geoderma.
796 337, 1067-1076.
797
798 Upadhayay, H.R., Bodé, S., Griepentrog, M., Huygens, D., Bajracharya, R.M., Blake,
799 W.H., Boeckx, P., 2017. Methodological perspectives on the application of compound-
800 specific stable isotope fingerprinting for sediment source apportionment. J. Soils
801 Sediments. 17(6), 1537-1553.
802
803 Vale, S.S., Fuller, I.C., Procter, J.N., Basher, L.R., Dymond, J.R., 2020. Storm event
804 sediment fingerprinting for temporal and spatial sediment source tracing. Hydrol.
805 Process. 34(15), 3370-3386.
806
807 Walling, D.E., Owens, P.N., Leeks, G.J., 1999. Fingerprinting suspended sediment
808 sources in the catchment of the River Ouse, Yorkshire, UK. Hydrol. Process. 13(7), 955-
809 975.
810